A A porous Zn(II)-coordination polymer based on tetracarboxylic acid exhibiting selective CO_2 adsorption and iodine uptake

Mürsel Arici[a,*], Tuğba Alp Arici[b], Hakan Demiral[c], Murat Taş[d] and Okan Zafer Yeşilel[a]

[a]Department of Chemistry, Faculty of Science and Letters, Eskişehir Osmangazi University, 26040 Eskişehir, Turkey

[b]Department of Chemical Technology, Emet Vocational School, Kütahya Dumlupınar University, 43700, Kütahya, Turkey

[c]Department of Chemical Engineering, Faculty of Engineering and Architecture, Eskişehir Osmangazi University, 26040 Eskişehir, Turkey

[d]Department of Science Education, Education Faculty, Ondokuz Mayıs University, 55139, Samsun, Turkey

Contents:

Table and Figure Captions

Fig. S7. (a) IR spectra of **2a** before and after I_2 adsorption in solution and vapor phase **(b)** PXRD patterns of **2a, 2a@I_2(solvent), 2a@I_2(vapor)** and **2a@I_2(desorption)**

Fig. S8. (a) I_2 release of **2a@I_2** (10 mg) into methanol (10 mL) with time **(b)** the curve of I_2 desorption *vs* time

Table S1. Selected bond distance (Å) and angle (°) data for **1**

Zn1–Zn1^{i}	3.0880 (4)	Zn1–N1	2.0090 (17)
Zn1–O1	2.0331 (14)	Zn1–O3^{iii}	2.0384 (14)
Zn1–O4^{ii}	2.0500 (15)	Zn1–O2^{i}	2.0508 (14)
O1–Zn1–Zn1^{i}	83.99 (5)	N1–Zn1–O4^{ii}	100.08 (7)
O1–Zn1–O4^{ii}	85.33 (7)	N1–Zn1–O3^{iii}	104.78 (7)
O1–Zn1–O3^{iii}	87.52 (7)	N1–Zn1–O2^{i}	99.55 (7)
O1–Zn1–O2^{i}	154.92 (7)	O3^{iii}–Zn1–Zn1^{i}	74.07 (5)
O4^{ii}–Zn1–Zn1^{i}	81.50 (5)	O3^{iii}–Zn1–O4^{ii}	155.12 (7)
O4^{ii}–Zn1–O2^{i}	86.10 (7)	O3^{iii}–Zn1–O2^{i}	90.45 (7)
N1–Zn1–Zn1^{i}	170.80 (5)	O2^{i}–Zn1–Zn1^{i}	71.44 (5)
N1–Zn1–O1	105.14 (7)		

Symmetry codes: (i) −x+3/2, −y+½, −z+2; (ii) x, −y+1, z+½; (iii) −x+3/2, y−½, −z+3/2; (iv) x, −y+1, z−½; (v) −x+1, −y+1, −z+1; (vi) −x+3/2, y+½, −z+3/2; (vii) −x+1, y, −z+3/2.

Table S2. Selected bond distance (Å) and angle (°) data for **2**

Zn1–Zn1^{i}	3.0826 (7)	Zn1–O1	2.036 (2)
Zn1–O4^{ii}	2.040 (3)	Zn1–O2^{i}	2.044 (3)
Zn1–O3^{iii}	2.059 (2)	Zn1–N1	2.007 (3)
O4^{ii}–Zn1–Zn1^{i}	84.56 (8)	O1–Zn1–O2^{i}	155.13 (12)
O4^{ii}–Zn1–O3^{iii}	155.19 (12)	O2^{i}–Zn1–Zn1^{i}	81.07 (8)
O4^{ii}–Zn1–O2^{i}	85.83 (14)	N1–Zn1–Zn1^{i}	170.83 (10)
O3^{iii}–Zn1–Zn1^{i}	71.09 (8)	N1–Zn1–O4^{ii}	104.61 (13)
O1–Zn1–Zn1^{i}	74.52 (8)	N1–Zn1–O3^{iii}	99.77 (12)
O1–Zn1–O4^{ii}	87.18 (13)	N1–Zn1–O1	105.56 (13)
O1–Zn1–O3^{iii}	90.73 (12)	N1–Zn1–O2^{i}	99.30 (13)
O2^{i}–Zn1–O3^{iii}	85.77 (13)		

Symmetry codes: (i) −x+3/2, −y+3/2, −z+1; (ii) −x+3/2, y+½, −z+3/2; (iii) x, −y+1, z−½; (iv) −x+3/2, y−½, −z+3/2; (v) x, −y+1, z+½; (vi) −x+1, −y+1, −z+1; (vii) −x+2, y, −z+3/2.

Table S3. Selected bond distance (Å) and angle (°) data for **2a@I_2**

Zn1–Zn1^{i}	3.0844 (19)	Zn1–N2	2.007 (8)
Zn1–O1	2.047 (6)	I1–I1^{vii}	2.54 (2)
Zn1–O3^{ii}	2.047 (6)	I1–I2	2.83 (3)
Zn1–O2^{i}	2.050 (6)	I2–I2^{viii}	2.60 (3)
Zn1–O4^{iii}	2.051 (6)		
O1–Zn1–O2^{i}	154.9 (3)	O2^{i}–Zn1–O4^{iii}	86.0 (3)
O1–Zn1–O4^{iii}	85.4 (3)	N2–Zn1–O1	105.4 (3)
O3^{ii}–Zn1–O1	87.4 (3)	N2–Zn1–O3^{ii}	105.1 (3)
O3^{ii}–Zn1–O2^{i}	90.7 (3)	N2–Zn1–O2^{i}	99.2 (3)
O3^{ii}–Zn1–O4^{iii}	155.2 (3)	N2–Zn1–O4^{iii}	99.7 (3)

Symmetry codes: (i) −x+1/2, −y+3/2, −z; (ii) −x+1/2, y+1/2, −z+1/2; (iii) x, −y+1, z−1/2; (iv) −x+1/2, y−1/2, −z+1/2; (vii) −x+1, −y+2, −z+1; (viii) −x+1, y, −z+1/2.

Table S4. Comparison of the I_2 uptake capacity (per formula unit) in selected iodine containing compounds

Compounds	**I_2 uptake capacity (per formula unit)**	**Reference**
TMU-16-NH_2	0.6	[1]
TMU-15	3	[2]
MIL-101-NH_2, CAU-1	0.71, 0.31	[3]
Compound 1	1.5	[4]
MOF 1’	4.2	[5]
JLU-Liu14	0.5	[6]
{[CuII(btz)]·0.5H_2O}$_n$	0.5	[7]
[Zn_3(DLlac)$_2$(pybz)$_2$]$_n$·	3	[8]
ZIF-8	1.25	[9]
HKUST-1	1.75	[10]
Azo-bridged porphyrin–phthalocyanine	2.90	[11]
{[Zn_2(μ_4-ao$_2$btc)(μ-pbix)$_2$]·2DMF·8H_2O}$_n$	1.47	[12]
{[Co_2(μ_8-abtc)(betib)]}$_n$	1.975	[13]
[Cd(L1)$_2$(ClO_4)$_2$]	2	[14]
{[Zn_2(μ_8-abtc)(betib)]}$_n$	**1.975**	**This work**

Table S5. Comparison of the iodine release rate of the selected compounds based on the calibration curve of standard iodine

Compounds	**Release rate/ mol L^{-1} min^{-1} ($\times 10^{-6}$)**	**Ref.**
$Cu_2(H_2O)_2(Cu_4I_4)_2(INA)_4(DABCO)_2 \cdot 2DMA$	0.288 (0.0875 mg /120 min)	[15]
JLU-Liu14b	0.5	[6]
$[(Cu_2I)Cu_2L_2(H_2O)_2]_2^{2+} \cdot 2NO_3^- \cdot 5DMF$	5.2	[16]
$[Cu_4I_3(DABCO)_2]I_3$	1.4	[17]
JLU-Liu32	2.3	[18]
JLU-31	0.85	[18]
{[$Zn_2(\mu_8$-abtc)(betib)]}	**0.595**	**This work**

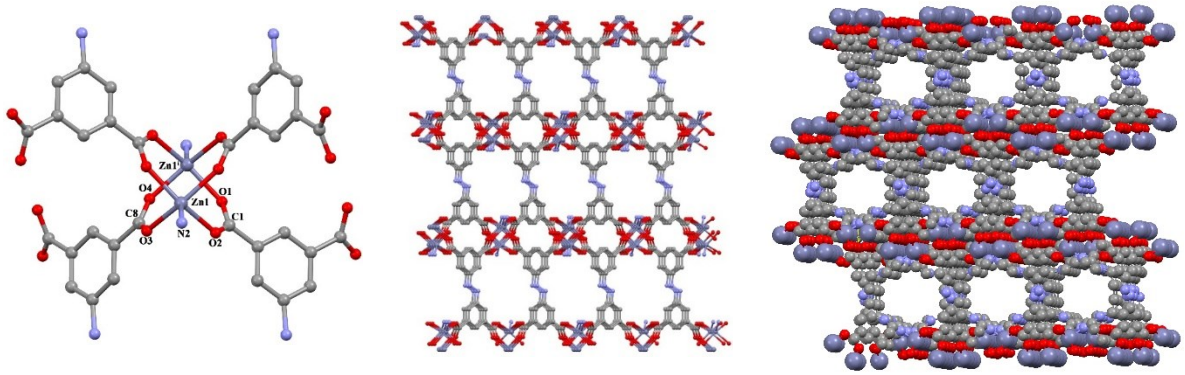

(a) **(b)** **(c)**

Fig. S1. (a) The coordination environments of the Zn(II) ions in the paddle-wheel cluster **(b)** View of the 3D framework of [Zn_2(abtc)] (1,4-betib ligands removed for clarity) **(c)** Space-filling mode of 3D structure in **1** and **2** along the c-axis

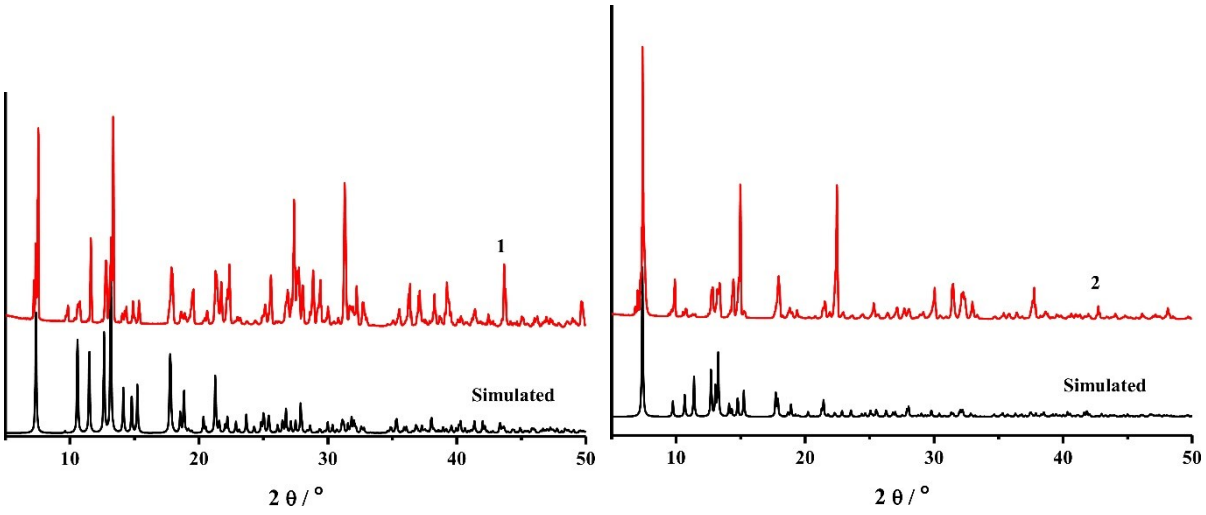

Fig. S2. PXRD patterns of simulated and as-synthesized compounds

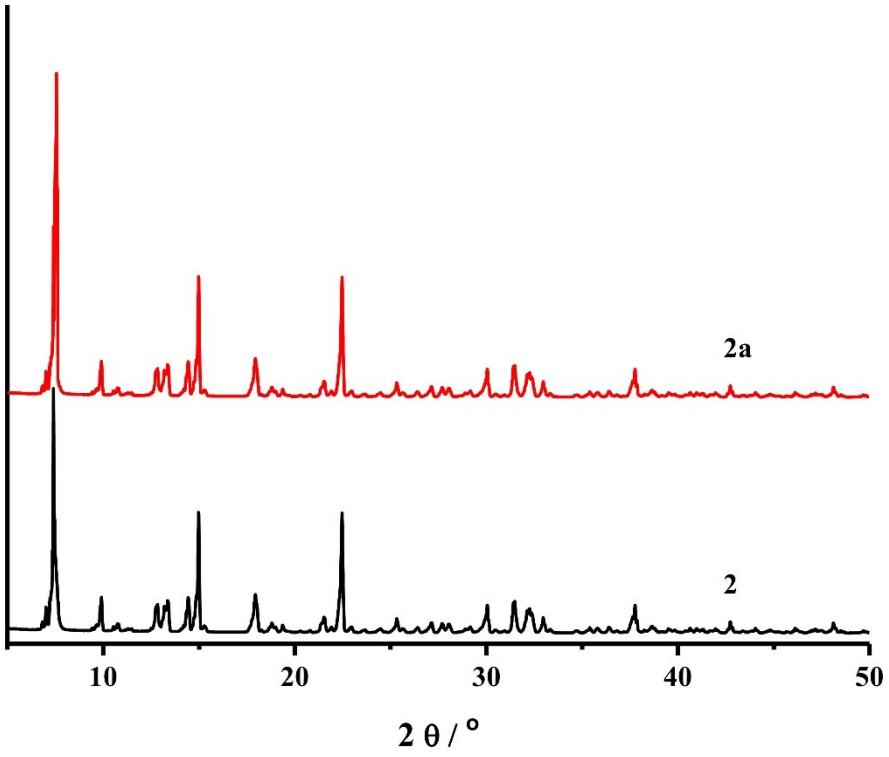

Fig. S3. PXRD patterns of compound **2** before and after fully activation at 140°C

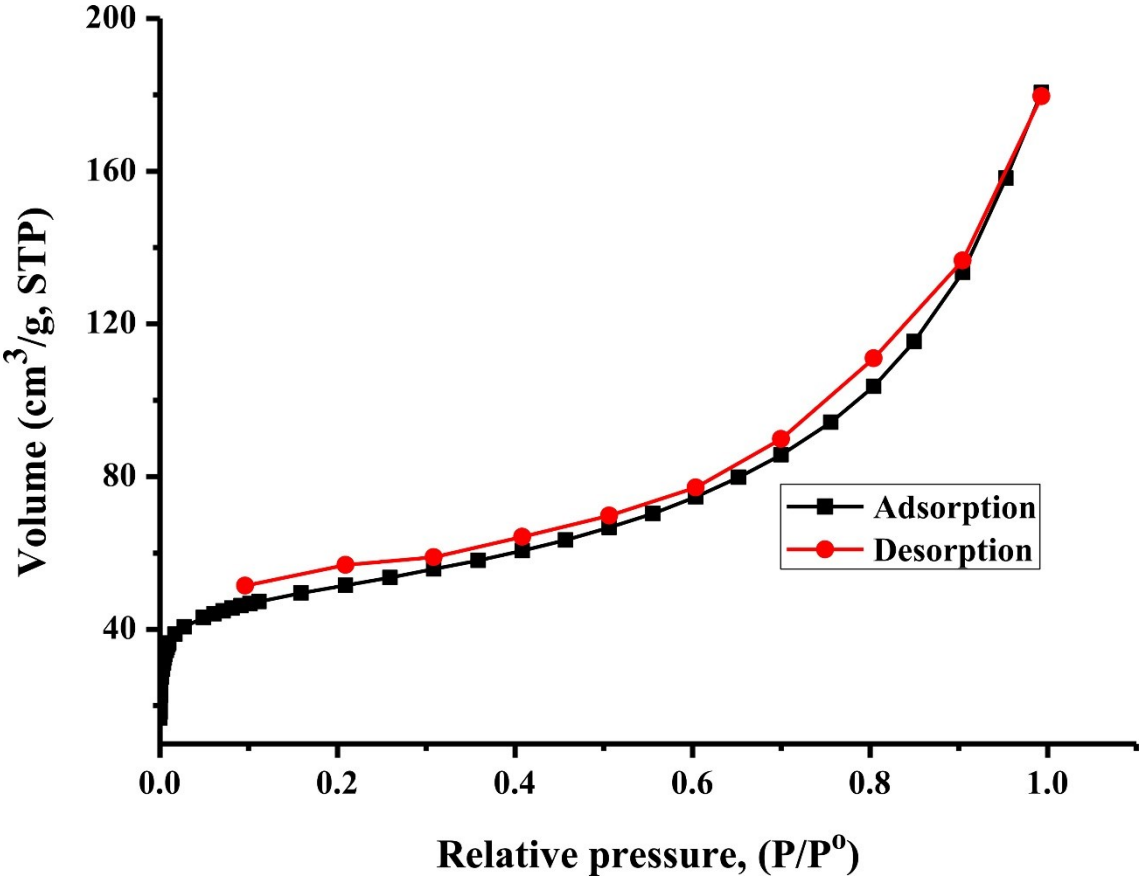

Fig. S4. N_2 adsorption-desorption isotherms of **2a** at 77 K

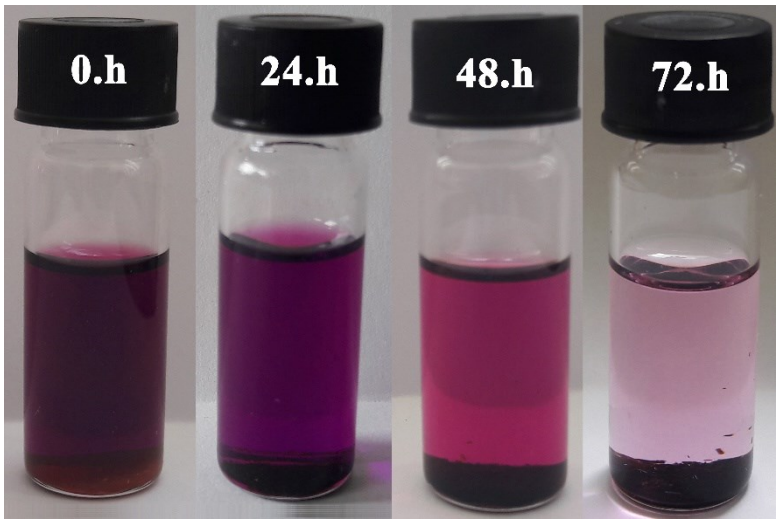

Fig. S5. The photographs of I_2 adsorption of **2a** in cyclohexane with time

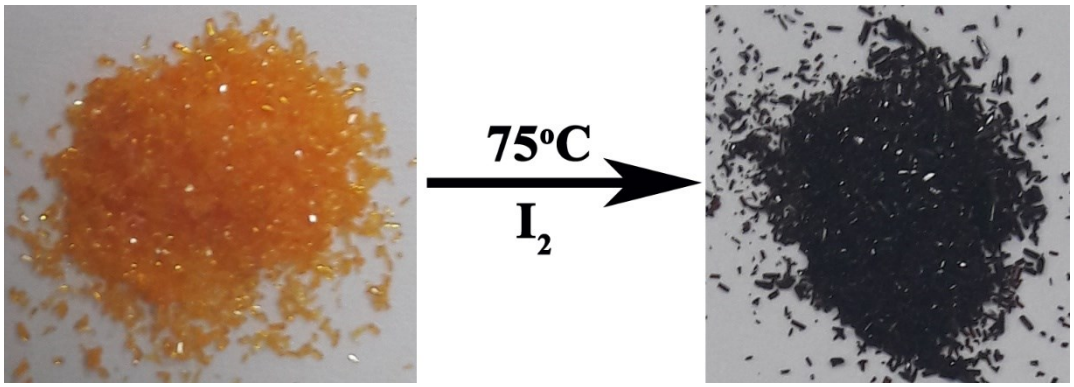

Fig. S6. The color change of **2a** after exposure to I_2 vapor at 75°C

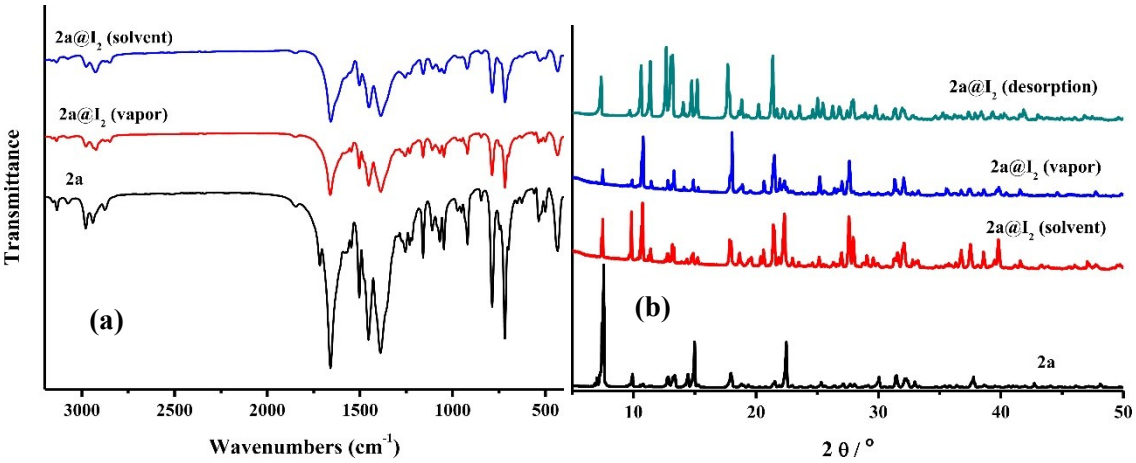

Fig. S7. (a) IR spectra of **2a** before and after I_2 adsorption in solution and vapor phase **(b)** PXRD patterns of **2a, 2a@I_2(solvent), 2a@I_2(vapor)** and **2a@I_2(desorption)**

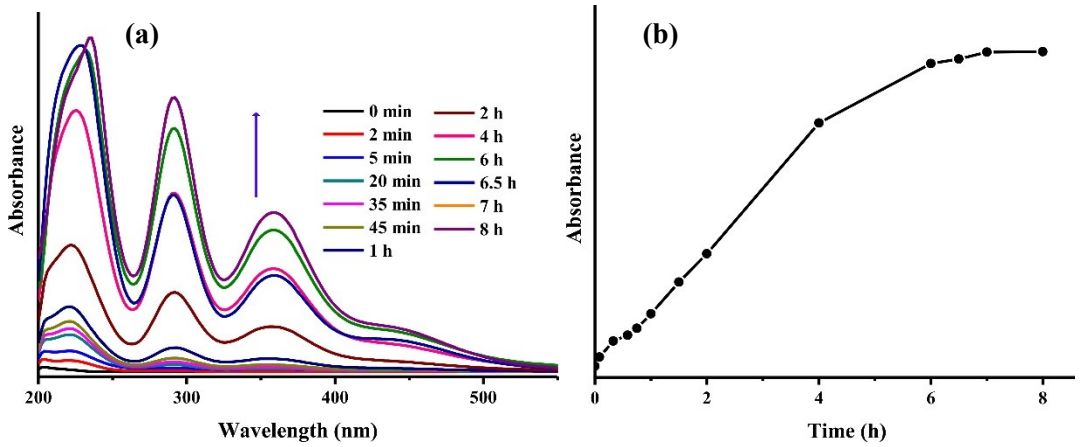

Fig. S8. (a) I_2 release of **2a@I_2** (10 mg) into methanol (10 mL) with time **(b)** the curve of I_2 desorption *vs* time

Notes and references

1. V. Safarifard and A. Morsali, *CrystEngComm*, 2014, **16**, 8660-8663.
2. L. Hashemi and A. Morsali, *CrystEngComm*, 2014, **16**, 4955-4958.
3. C. Falaise, C. Volkringer, J. Facqueur, T. Bousquet, L. Gasnot and T. Loiseau, *Chem. Commun.*, 2013, **49**, 10320-10322.
4. Y. Q. Hu, M. Q. Li, Y. Wang, T. Zhang, P. Q. Liao, Z. Zheng, X. M. Chen and Y. Z. Zheng, *Chem. Eur. J.*, 2017, **23**, 8409-8413.
5. A. K. Chaudhari, S. Mukherjee, S. S. Nagarkar, B. Joarder and S. K. Ghosh, *CrystEngComm*, 2013, **15**, 9465-9471.
6. J. Wang, J. Luo, X. Luo, J. Zhao, D.-S. Li, G. Li, Q. Huo and Y. Liu, *Cryst. Growth Des.*, 2015, **15**, 915-920.
7. P. Cui, L. Ren, Z. Chen, H. Hu, B. Zhao, W. Shi and P. Cheng, *Inorg. Chem.*, 2012, **51**, 2303-2310.
8. M.-H. Zeng, Q.-X. Wang, Y.-X. Tan, S. Hu, H.-X. Zhao, L.-S. Long and M. Kurmoo, *J. Am. Chem. Soc.*, 2010, **132**, 2561-2563.
9. D. F. Sava, M. A. Rodriguez, K. W. Chapman, P. J. Chupas, J. A. Greathouse, P. S. Crozier and T. M. Nenoff, *J. Am. Chem. Soc.*, 2011, **133**, 12398-12401.

10. D. F. Sava, K. W. Chapman, M. A. Rodriguez, J. A. Greathouse, P. S. Crozier, H. Zhao, P. J. Chupas and T. M. Nenoff, *Chem. Mater.*, 2013, **25**, 2591-2596.

11. H. Li, X. Ding and B. H. Han, *Chem. Eur. J.*, 2016, **22**, 11863-11868.

12. M. Arıcı, O. Z. Yeşilel, M. Tas and H. Demiral, *Inorg. Chem.*, 2015, **54**, 11283-11291.

13. M. Arici, O. Z. Yeşilel, M. Taş and H. Demiral, *Cryst. Growth Des.*, 2017, **17**, 2654-2659.

14. Q.-K. Liu, J.-P. Ma and Y.-B. Dong, *Chem. Commun.*, 2011, **47**, 7185-7187.

15. J.-H. Liu, J. Zhang, D. Zhao, L.-D. Lin, Y.-Q. Sun, X.-X. Li and S.-T. Zheng, *CrystEngComm*, 2020, **22**, 821-828.

16. J. Yuan, J. Li, L. Kan, L. Zou, J. Zhao, D.-S. Li, G. Li, L. Zhang and Y. Liu, *C Cryst. Growth Des.*, 2018, **18**, 5449-5455.

17. B. Xin, G. Zeng, L. Gao, Y. Li, S. Xing, J. Hua, G. Li, Z. Shi and S. Feng, *Dalton Trans.*, 2013, **42**, 7562-7568.

18. S. Yao, X. Sun, B. Liu, R. Krishna, G. Li, Q. Huo and Y. Liu, *JJ. Mater. Chem. A*, 2016, **4**, 15081-15087.